

# Two-dimensional disordered lattice solitons

Nikolaos K. Efremidis

Department of Applied Mathematics, University of Crete, 71409 Heraklion, Crete, Greece  
(nefrem@tem.uoc.gr)

Received December 9, 2008; accepted January 10, 2009;  
posted January 27, 2009 (Doc. ID 105042); published February 23, 2009

We investigate families of optical solitons supported by two-dimensional disordered lattices. The linear modes of the system are identified, and their eigenvalues are arranged in a band structure. Introducing Kerr nonlinearity, we find that families of solitons originate from linear modes. Such solutions, depending on the eigenvalue of the supporting linear mode, as the power increases may become less localized/delocalized via resonant interactions with the modes of the linearized lattice. In addition, families of highly confined solitons exist in every waveguide of the lattice and for both signs of the nonlinearity. © 2009 Optical Society of America

OCIS codes: 190.6135, 190.0190, 190.4420.

In recent years there has been an increased interest in the study of periodic waveguide structures, including waveguide arrays, optically induced lattices, and fiber arrays [1,2]. Such systems are known to support extended Floquet–Bloch modes [3]. Anderson showed that by introducing disorder in periodic configurations, the linear modes may become spatially localized [4]. The transition between localized and extended modes depends on the dimensionality of the problem as well as on the position of the eigenvalue inside the band structure. The main application of this theory is to investigate electrical transport phenomena in condensed matter physics [5–8].

Optical waveguide lattices provide an excellent environment for the study of the competition between disorder and nonlinearity. Experimentally, light propagation in disordered two-dimensional (2D) arrays of mutually coupled fibers is reported [9], while in [10] an experimental observation of Anderson localization in a perturbed periodic potential is observed. The linear and the nonlinear evolution in an Anderson model of optical waveguides has also been investigated in [11]. Theoretically, discrete nonlinear Schrödinger (NLS) type models have been examined for the study of discrete breather formation in random lattices [12]. Recently, a lattice NLS equation modeling disordered waveguide arrays in one dimension has been studied [13]. In particular, families of disordered lattice solitons (DLSs) were analyzed and categorized to a few classes with the same qualitative properties.

In this Letter, we investigate the properties of solitons supported by 2D disordered lattices. We find that each family of solutions shares common properties with a large number of families (forming a class). Thus, by examining typical examples from each class, one can understand the behavior of all the families included. Families of DLS originate from linear modes, which as the power increases may become less localized/delocalized owing to resonant interactions with the modes of the linearized lattice. Interestingly enough these latter modes do not have a low power threshold, in contrast with 2D solitons in periodic media [14]. In addition, families of highly confined DLS exist in each waveguide of the lattice and

for both signs of the nonlinearity. All of these families of solutions, except one, exhibit a lower power threshold.

In the paraxial limit, the propagation of an optical wave in a 2D Kerr medium in normalized units is given by

$$i\psi_z + \psi_{xx} + \psi_{yy} + V(x,y)\psi + \gamma|\psi|^2\psi = 0, \quad (1)$$

where  $\psi$  is the complex amplitude of the field,  $x$ ,  $y$ , and  $z$  are the transverse and the propagation coordinates,  $\gamma$  is the Kerr coefficient, and the potential  $V(x,y)$  is proportional to the refractive index. In our simulations we use a square domain  $-L/2 \leq x, y \leq L/2$  with  $L=16$ . The results are not affected by the type of boundary conditions used (periodic or zero); however, periodic boundaries are preferred to avoid surface effects. Equation (1) conserves the total power  $P = \int |u|^2 dx dy$  and the Hamiltonian. The disordered potential  $V(x,y)$  can model the index distribution in optically induced lattices [15,16], fiber arrays [9], or waveguides in bulk glasses [17]. In particular, we choose  $V = V_p + rV_d$ , where

$$V_p = - (V_0/2)(\cos^2(\pi x/2) + \cos^2(\pi y/2)) \quad (2)$$

is a square periodic (each side is equal to 2),

$$V_d = \frac{1}{V_m} \sum_{m,j_1,j_2=1}^{10} \alpha_{j_1,j_2} \sin((2\pi j_1 x/L) + \phi_{x,j_1,j_2}) \sin((2\pi j_2 y/L) + \phi_{y,j_1,j_2}) \quad (3)$$

is a random potential, and  $\alpha_{j_1,j_2}$ ,  $\phi_{x,j_1,j_2}$ ,  $\phi_{y,j_1,j_2}$  are realizations of the uncorrelated random variables  $A$ ,  $\Phi_x$ ,  $\Phi_y$ , obeying uniform distributions with  $-1 \leq A \leq 1$ ,  $0 \leq \Phi_x, \Phi_y \leq 2\pi$ .  $V_m$  is chosen such that  $\max(|V_d|) = 1$ , while  $r$  is a deterministic real parameter that determines the degree of disorder in the lattice. Assuming stationary solutions of the form  $\psi = u(x,y)\exp(-iEz)$  the real nonlinear eigenvalue problem  $(E + V(x))u + u_{xx} + u_{yy} + \gamma u^3 = 0$  is derived. Solutions of this latter equation are obtained using Newton's iteration scheme.

In Fig. 1(a) a typical disordered potential of 64 waveguides is shown for  $V_0=20$  and  $r=6$ . Through

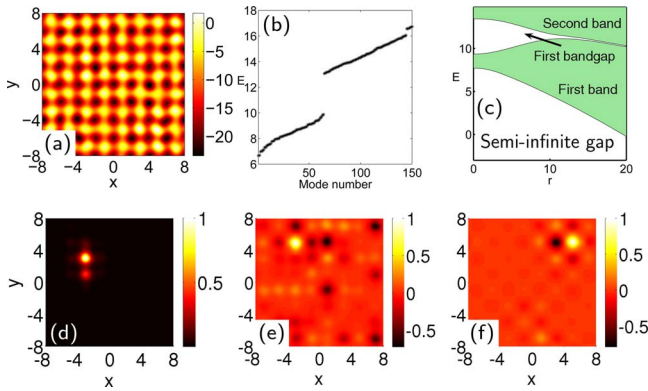


Fig. 1. (Color online) (a) Disordered index potential. (b) Eigenvalues of the linear modes (enumerated in increasing  $E$  order) forming a band structure. (c) Regions of bands (shaded, green online) and bandgaps (white) as a function of the disorder parameter  $r$ . (d)–(f) Linear modes 1, 38, and 64 with  $E_1=6.67$ ,  $E_{38}=8.69$ , and  $E_{64}=9.88$ , respectively.

the rest of this Letter we are going to use this particular configuration unless stated otherwise. The linear modes and their eigenvalues are derived numerically. In Fig. 1(b) the first 150 eigenvalues ( $E_{j,j} = 1, \dots, 150$ ) forming a band structure are shown in increasing  $E$  order. The potential depth  $V_0=20$  is chosen so that a well-defined complete bandgap opens up between the first and the second band. Notice that the first band contains as many linear modes as the lattice waveguides (64). Typical profiles of the linear modes are shown in Figs. 1(d)–1(f). Modes located in the first band edges are in general narrower as compared to modes in the middle of the band. Furthermore, linear modes become less localized as  $E$  increases. We computed the bandgap structure as a function of the disorder parameter  $r$  and found that the bands become wider and the bandgaps narrower as  $r$  increases. In Fig. 1(c) the average band edges taken over ten different disordered potential realizations are shown. For  $r \geq 12$  essentially the bandgap disappears.

Families of DLS that are highly confined in one waveguide exist for both signs of the nonlinearity and for every waveguide in the lattice. In the self-focusing case, such modes have eigenvalues located in the semi-infinite bandgap of the band structure. In Fig. 2(a) a typical power versus eigenvalue diagram is shown. The corresponding DLS for  $E=5$  is presented in Fig. 2(b). In Fig. 2(c) the  $P$ – $E$  curves of all 64 families of solutions are depicted. All the families of solutions except one exhibit lower power thresh-

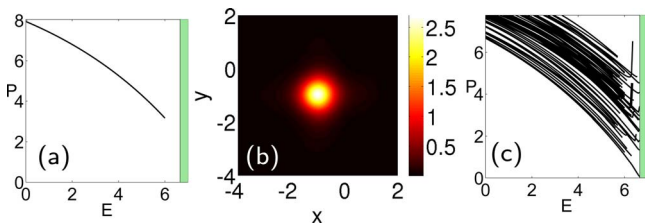


Fig. 2. (Color online) Self-focusing DLS highly confined in a single waveguide of the lattice. (a) Typical  $P$ – $E$  curve and (b) corresponding field amplitude for  $E=5$ . (c)  $P$ – $E$  curves of all 64 families.

olds. (They also exhibit upper power thresholds, since as  $E$  decreases the solutions asymptotically take the Townes soliton profile.) The only family of solutions that does not have a lower power threshold asymptotically takes the form of the linear mode 1 as  $E \rightarrow E_1$  (and  $P \rightarrow 0$ ).

In a similar fashion, in the self-defocusing case, 64 different families of DLS exist. Each one of these families is highly confined in a different waveguide of the lattice. A necessary requirement for such solutions to exist is the presence of a wide-enough bandgap. The DLS eigenvalues reside in the first bandgap as well as in the second band [Fig 3(a)]. When the eigenvalue is located inside the bandgap the DLSs are strongly confined into one waveguide, and their amplitude phase-difference between first neighbor waveguides is  $\pi$ . However, as  $E$  increases and enters the second band the solutions exhibit bifurcations with linear modes and, as a result, they become broader/delocalized. All the families of solutions except one exhibit a lower power threshold. The only family of solutions that does not have a lower power threshold takes the form of linear mode 64 [shown in Fig. 1(f)] as  $E \rightarrow E_{64}$  and  $P \rightarrow 0$ .

Families of DLS can also originate from linear modes. For small-enough focusing or defocusing nonlinearity, all the linear modes exist with slight modifications in their shape. Since  $P \rightarrow 0$  as  $E \rightarrow E_j$  such families of solutions do not have lower power thresholds, in contrast with 2D solitons in periodic lattices. For stronger nonlinearity DLSs may resonantly interact with modes of the linearized equation, leading to the formation of more complicated structures. The number of possible resonant interactions depends on the location of the DLS eigenvalue inside the band structure and the sign of the nonlinearity. In particular, a DLS originating from linear mode  $n$  might resonantly interact with modes  $1 \leq j \leq n-1$  if  $\gamma=1$  and with modes  $j \geq n+1$  if  $\gamma=-1$ . Linear mode 1 with  $\gamma=1$  does not exhibit resonant interaction. This family of solutions is identical with the one discussed above that is highly confined in a single waveguide and does not have a lower power threshold. Similar arguments apply for linear mode 64 in the case of self-defocusing nonlinearity; it does not exhibit resonant interactions before it enters the first gap and is identical with the family of highly confined DLS with  $\gamma=-1$  that does not have a lower power threshold.

A typical example of a self-focusing family of solutions originating from a linear mode is shown in Fig. 4. Linear mode 4 [Fig. 4(b)] exhibits a dipole structure with most of the power localized on waveguides

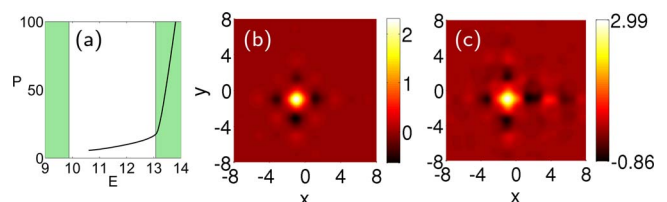


Fig. 3. (Color online) Defocusing family of DLS highly confined in a single waveguide of the lattice (a)  $P$ – $E$  curve. (b) and (c) Field amplitude for  $E=10.6, 13$ .

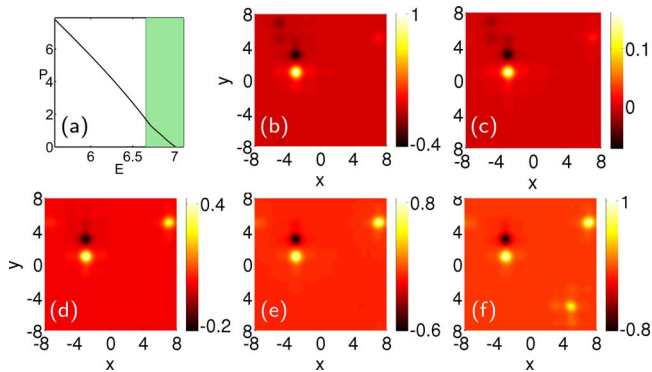


Fig. 4. (Color online) Family of self-focusing DLS originating from linear mode 4. (a)  $P-E$  curve, (b) linear mode with  $E_4=7.017$ , and (c)–(f) DLS for  $E=7.007, 6.947, 6.727, 6.572$ , respectively.

(3, 5) and (3, 6) of the array (the numbers denote discrete waveguide coordinates along  $x$  and  $y$ ). For a small-enough nonlinearity the resulting dipole DLS maintains its shape [Fig 4(c)]. Owing to a resonant interaction with linear mode 3 with eigenvalue  $E_3=6.985$  and maximum intensity on waveguide (8, 7), the amplitude in this latter waveguide is increased for  $E \geq E_3$  [Fig 4(d)]. As  $E$  further decreases the DLS interacts with linear mode 2 with eigenvalue  $E_2=6.709$ , which is strongly localized on waveguide (7, 2) of the array [Fig. 4(f)]. Notice that linear mode 1, shown in Fig. 1(d), has a maximum amplitude in the same lattice sites with linear mode 4. We did not notice any significant change in the amplitude of this family of DLS due to a bifurcation with linear mode 1.

Subsequent resonant interactions of solitons with modes of the linearized equation can result in the eventual expansion/delocalization of the DLS. An example is shown in Fig. 5, where a family of solutions originating from linear mode 64 [Fig. 1(f)] is depicted. As  $E$  decreases the DLS resonantly interacts with linear modes 63, ..., 1. After several resonant interactions the mode becomes delocalized [Fig. 5(c)].

Notice that following [13] we can classify the families of DLS bifurcating from linear modes into three different classes. The first contains solutions that do

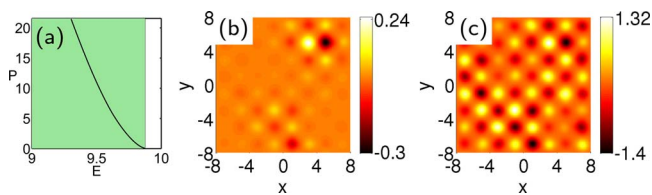


Fig. 5. (Color online) Self-focusing family of DLS originating from linear mode 64. (a)  $P-E$  curve. (b) and (c) Nonlinear modes for  $E=9.85$  and  $9.2$ , respectively.

not exhibit resonant interactions. The second class contains soliton families that bifurcate with linear modes but maintain a localized shape inside the gap. The third class contains soliton families that originate from linear modes and for strong nonlinearity turn delocalized. Finally, a fourth class of solutions contains families that have a lower power threshold and are strongly localized in the gaps.

In conclusion, we have studied families of 2D solitons supported by an NLS equation with disordered potential modeling waveguide lattices. We found that, for both signs of the nonlinearity, families of highly confined DLS exist in each waveguide of the lattice. In addition, families of DLS originate from each linear mode and may exhibit resonant interactions with the linear modes of the linearized spectrum, leading to broadening of the soliton profile. Interestingly enough, these latter families of solutions do not exhibit power thresholds.

## References

1. D. N. Christodoulides, F. Lederer, and Y. Silberberg, *Nature* **424**, 817 (2003).
2. F. Lederer, G. I. Stegeman, D. N. Christodoulides, G. Assanto, M. Segev, and Y. Silberberg, *Phys. Rep.* **463**, 1 (2008).
3. C. Kittel, *Introduction to Solid State Physics* (Wiley, 1986).
4. P. Anderson, *Phys. Rev.* **109**, 1492 (1958).
5. P. A. Lee and T. V. Ramakrishnan, *Rev. Mod. Phys.* **57**, 287 (1985).
6. D. Belitz and T. R. Kirkpatrick, *Rev. Mod. Phys.* **66**, 261 (1994).
7. J. D. Maynard, *Rev. Mod. Phys.* **73**, 401 (2001).
8. P. Sheng, *Introduction to Wave Scattering, Localization and Mesoscopic Phenomena* (Springer, 2006).
9. T. Pertsch, U. Peschel, J. Kobelke, K. Schuster, H. Bartelt, S. Nolte, A. Tünnermann, and F. Lederer, *Phys. Rev. Lett.* **93**, 053901 (2004).
10. T. Schwartz, G. Bartal, S. Fishman, and M. Segev, *Nature* **446**, 52 (2007).
11. Y. Lahini, A. Avidan, F. Pozzi, M. Sorel, R. Morandotti, D. N. Christodoulides, and Y. Silberberg, *Phys. Rev. Lett.* **100**, 013906 (2008).
12. G. Kopidakis and S. Aubry, *Phys. Rev. Lett.* **84**, 3236 (2000).
13. N. K. Efremidis and K. Hizanidis, *Phys. Rev. Lett.* **101**, 143903 (2008).
14. N. K. Efremidis, J. Hudock, D. N. Christodoulides, J. W. Fleischer, O. Cohen, and M. Segev, *Phys. Rev. Lett.* **91**, 213906 (2003).
15. N. K. Efremidis, S. Sears, D. N. Christodoulides, J. W. Fleischer, and M. Segev, *Phys. Rev. E* **66**, 046602 (2002).
16. J. W. Fleischer, M. Segev, N. K. Efremidis, and D. N. Christodoulides, *Nature* **422**, 147 (2003).
17. T. Pertsch, U. Peschel, F. Lederer, J. Burghoff, M. Will, S. Nolte, and A. Tünnermann, *Opt. Lett.* **29**, 468 (2004).